View metadata, citation and similar papers at core.ac.uk
brought to you by CORE
provided by International Journal on Advanced Science, Engineering and Information Technology

International Journal on Advanced Science Engineering Information Technology

Vol.10 (2020) No. 1
ISSN: 2088-5334

Improving the Accuracy of Ship Resistance Prediction Using Computational Fluid Dynamics Tool

Van Chinh Huynh[#], Gia Thai Tran[*]

[#]*Ho Chi Minh City University of Transport, Ho Chi Minh City, Vietnam*

[*]*Nha Trang University, Khanh Hoa, Vietnam*
E-mail: thaitg@ntu.edu.vn

***Abstract*— The ship resistance prediction using CFD tool has become an accepted method over the last decade; however, the CFD-based ship resistance results are not always accurate. This paper presents the approach of determining the input parameters of the CFD solution for ship resistance prediction, including of size and boundary conditions of the computational domain, and parameters of turbulent model in accordance with the geometric characteristics of hull to improve the accuracy of CFD-based resistance values for a specific ship type. Two same type of fishing vessels named FAO 72 and FAO 75 which are tested in towing tank are chosen as the computed ship to apply this approach for resistance prediction accurately. The CFD-based resistance results of these vessels are compared with corresponding model testing results to analyze accuracy and reliability of this approach as well as discussing the effect of the initial parameters of the CFD solution on the resistance results as mentioned. The research results shown that the accuracy of three dimensions (3D) model of computational ship, the appropriate values of computational domain size and turbulent model parameters for resistance prediction using CFD are the input factor to improve the accuracy of resistance values. Especially the specific values of computational domain size and turbulent model parameters are presented in this paper will be the input parameters to predict the resistance using CFD for the fishing vessels with the same geometric characteristics as the computed ship.**

***Keywords*— CFD; resistance; input parameter; accurate prediction; FAO.**

I. INTRODUCTION

The resistance prediction is one of the important problems in the ship design process and is also the basis of solving several critical practical problems such as calculating the main engine power and propeller under the hull, optimizing of the hull form to achieve the minimum resistance results. Up to now, in addition to traditional ship model test in towing tank, Computational Fluid Dynamics (CFD) has widely used to predict resistance and resolve complex problems in ship hydrodynamics [1], in which the flow around a hull is usually governed and computed with so-called Navier-Stokes equations that applied for the dynamics of Newtonian fluids [2], [3]. However, these equations cannot be solved in the turbulent case so when turbulences are important or significant, a modified form of Navier-Stokes equations in which the quantities dependent on time and space will be calculated according to their average quantities that are independent of time and space should be used [4]. They are called Reynold Averaged Navier-Stokes Equations were known as the famous RANS method in CFD [5]. However, RANS equations are still not enough to close system of equations governed the flow around a hull so adding additional equations which come from appropriate turbulence model to close the system of equations Two standard k-ε and k- ω models of turbulences were usually applied to predict resistance using CFD but they have proved to be inaccurate in the flow separation region; therefore, the turbulent model named Sheer Stress Transport (SST) k-ω has been widely used in most current works on CFD-based resistance prediction [6]. This turbulent model is a conglomeration of the robust and accurate formulation of the standard k-ω model in the near-wall region with the standard k-ε model in the far-field so they are more accurate and reliable [7]. The mathematical explanations of this turbulent model can be found in relevant specialized references [8].

There have been many theoretical and experimental works on application CFD to predict ship resistance. Du et al. [9] performed and made an intensive review on various types of resistance for the Wigley parabolic hull based on ITTC 1957 Model-ship Correlation line and using RANSE simulation. Petros Voxakis at Massachusetts Institute Technology (MIT) used DTMB-5415 model on resistance computation using standard turbulent model k-ε on RANS simulation and CFD software namely STAR-CCM$^+$ [4]. Lee et al. [7] used the Series 60 model on resistance calculation by CFD codes.

Son et al. [5] investigated frictional resistance using another type of ship model. Previously one research work by Chang et al. [10] and one conference by Zang et al. [11] were presented for the computational analysis of the flow around of ships. Computations of the resistance of KCS (Kriso Container Ship), DTC (Duisburg Test Case) and some other models using turbulent on RANS simulation and CFD software such as OpenFOAM were performed by Luo et al. [12], Diez et al. [8]. As a result of our review of the research relating to applying CFD to predict the ship resistance, it has been shown that there are several comments as follows:

The CFD theory with several different computation methods can be found in many specialized references. However, most current research on CFD-based resistance prediction have used the Reynold Averaged Navier-Stokes Equations known as famous RANSE in CFD with the turbulent model named (Sheer Stress Transport) SST k-ω combined of two standard turbulent models named k-ε model and k-ω model applied for a three-dimensional steady, incompressible and viscous turbulent flow around the given ship hulls [13]. The mathematical explanations can be found in many related specialized references but it is found that the parameters of this turbulent model, including turbulence kinematic energy (k) and turbulence specific dissipation, are (ω) have a greatly affected to the accuracy and reliability of the resistance values but there are not many research works shown how to determine these parameters for a specific ship.

Most of the ships that have been used to compute resistance using the CFD method are available hulls such as Wigley, serri 60, KCS, DTMB-5415, DTC etc [14]. They are all cargo ships with a bulbous bow, massive bow flare, large stern overhang and transom, and massive parallel middle body. Hull geometry and model test results of resistance are also publicly available since the accuracy of three dimensions model (3D model) of computational ship and the values of the necessary parameters, it so-called the initial parameters of CFD solution including the size of computational domain, the boundary conditions, parameters of turbulent model on RANS simulation have not usually presented in relevant researches. In the specific application research, the accuracy of the CFD-based resistance values is usually analyzed and evaluated by comparing resistance results computed from CFD and corresponding model test results [11]. However, the accuracy of CFD-based resistance values is often uncertain and very different model test values since depending on the accuracy of the computational model and value of the above initial parameters [12].

The above comments can show that it is not easy to predict the resistance for a specific type of ship accurately since the accuracy is irrelevant to the computational ship model and values of the above initial parameters. Therefore, an approach to obtain the CFD-based ship resistance values accurately based on ensuring the accuracy of the 3D model of the computational ship and determining the value of initial parameters of the CFD solution following the geometric characteristics of the specific form of given hulls were presented in this paper. The fishing vessel named FAO 75 which is collected and tested in towing tank by Food and Agriculture Organization of the United Nations (FAO) is chosen as the computational ship to predict resistance using CFD and apply this approach for improving the accuracy of corresponding resistance values computed from CFD. Their lines are shown in Figure 1 with a bulbous bow, large overhang and cruiser, small parallel middle body. The model test results in a towing tank are published in FAO's references [15].

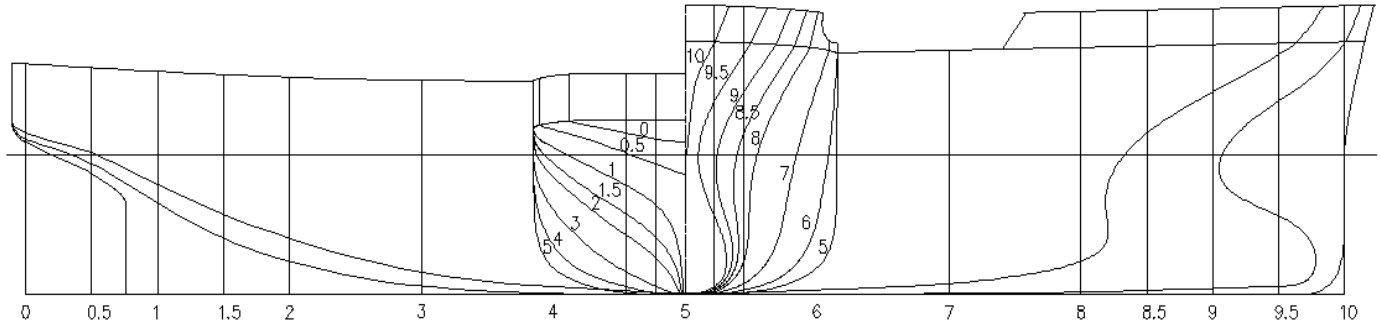

Fig. 1 FAO 75 fishing vessel's lines[15]

II. Materials and Method

The 3D model is the input of CFD problems so its accuracy has dramatically affected the CFD-based values and the model surface is smooth with the accuracy is high which can reduce the error of the simulation results. Mainly, the ship hulls are usually formed by many complex surfaces so generating and ensuring the necessary accuracy of their 3D model when comparing with the corresponding real ship is always not simple. Therefore, the 3D model of the computational ship should be created using the ship design software so that it is possible to use the software's built-in tools for adjusting and ensuring the required accuracy based on comparing the value of the geometric parameters between generated 3D model and corresponding real ship. In case study, the 3D models of computational hulls were created and adjusted from their lines in Figure 1 using ship design software named AutoShip so that the deviations of geometric parameters between 3D model and the corresponding real hulls are in limit which is usually less than 3% as are shown in Figure 2 and Table 1.

As usual, the 3D ship model will be saved under STL (standard stereolithographic) file format to import OpenFoam what the known CFD software is usually used to predict the ship resistance.

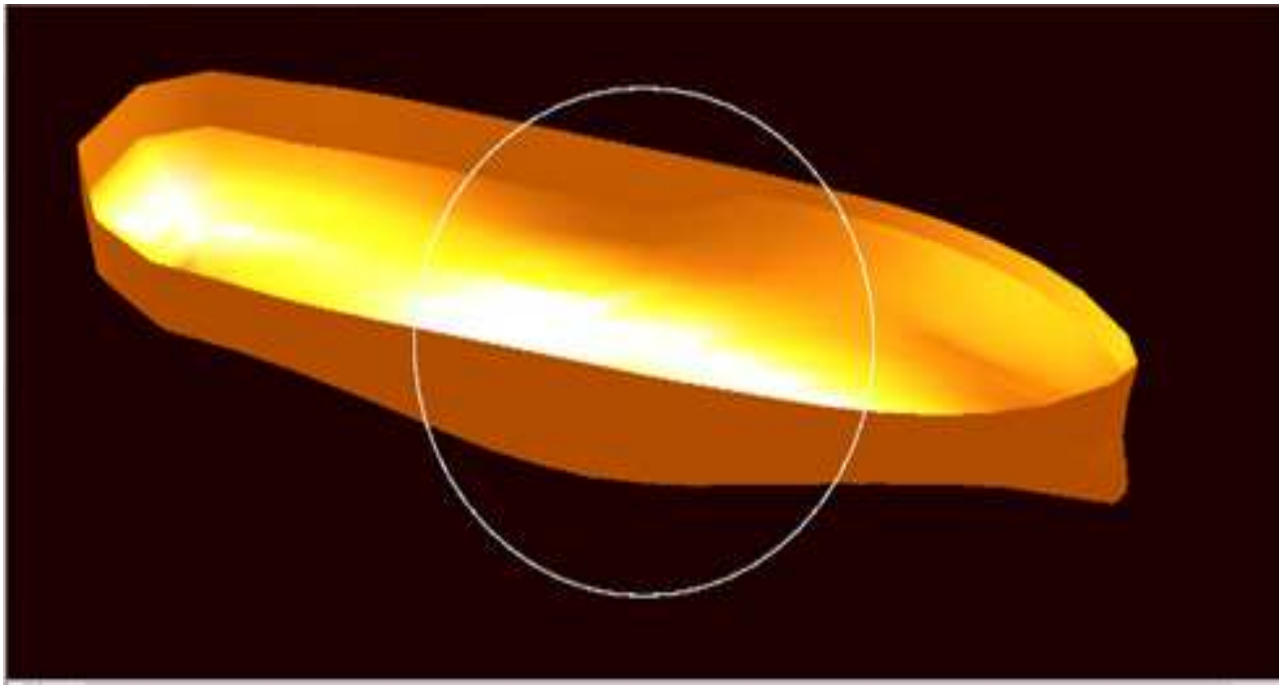

Fig. 2 The model and the geometric parameter of FAO 75 vessel in AutoShip software

TABLE 1
COMPARATIVE THE GEOMETRIC PARAMETERS OF 3D MODEL OF FAO 75 IN AUTOSHIP SOFTWARE AND REAL SHIP

Ship Parameters	Notation	Unit	FAO 75	FAO 75 Model in AutoShip software	Deviation (%)
Length of water line	L_{WL}	m	44.200	44.146	0.12
Breadth of waterline	B_{WL}	m	10.400	10.400	0.00
Depth	D	m	4.57	4.57	0.00
Displacement Volume	∇	m^3	1130.00	1127.20	0.25
Longitudinal Center of Buoyance	LCB	m	1.223	1.218	0.41
Block Coefficient	C_B	-	0.524	0.524	0.00
Prismatic Coefficient	C_P	-	0.581	0.590	-1.55
Wetter Surface Area	Ω	m^2	598.00	590.26	-1.29

III. RESULTS AND DISCUSSIONS

A. Determining Size and Boundary Conditions of Computational Domain

Computational domain refers to a rectangular box space that is limited by boundary conditions surrounding the ship hull to perform the numerical simulation in resistance prediction of the given hull using the CFD tool. The mathematical and physical explanations of the size and the boundary conditions of the computational domain can be found in [16], in which the boundary conditions in predicting resistance using CFD are chosen following the most common conditions named inlet, outlet, side, bottom, wall and symmetry plane as shown in Figure 3.

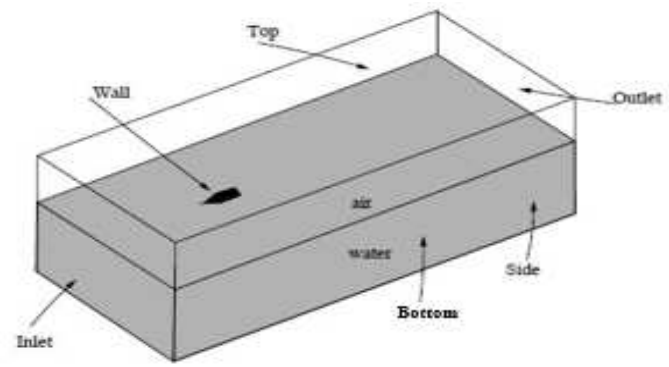

Fig. 3 Size and position of boundary conditions of the computational domain

In this case, a uniform flow with the free surface elevation was given and fixed at the inlet boundary condition, a hydrostatic pressure, which was calculated assuming an undisturbed free surface, was used for downstream at the outlet boundary condition; smooth walls with a free-slip were assumed for the top, bottom and sides. Smooth walls with a nonslip condition were assumed for in the entire hull. The hull was cut in the symmetry plane to speed up calculation. In the computational domain, two fluids were modeled including water and air. The water level was set to a draught of the vessel in the model scale [17].

It was found that the smaller the size of the computation domain the less the computation time of the simulation process but the CFD-based resistance prediction results may be changed due to the boundary condition effect. As a result, the appropriate size of the computational domain can be determined based on ensuring the size of the computational domain is minimum and the CFD-based resistance prediction results are stable and unchanged. Since then it is suggested how to determine the appropriate size of the computational domain for the given ship model. Preliminary estimating the size and boundary positions of the computational domain under the ship model based on existing recommendations or references. It is so-called as the initial variant. The size of the computational domain is usually determined according to the length overall (L_{OA}) or the length between the perpendiculars (L_{PP}) of the ship model. Some of the recommendations and references on the size of the computational domain in resistance prediction using CFD are shown in Table 2. The initial size variant of the computational domain should be chosen with the furthest boundary locations based on the boundary locations given in the recommendations.

Determining the appropriate size variant of the computational domain by changing the distance between each boundary and ship model of the initial variant gradually while keeping the positions of the remaining boundaries is unchanged until the CFD-based resistance prediction result is stable and unchanged.

TABLE II
RECOMMENDATIONS OF SIZE AND BOUNDARY POSITIONS OF COMPUTATIONAL DOMAIN IN CFD-BASED RESISTANCE PREDICTION

Recommendation	Range apply	Size and positions of boundary conditions of the computational domain, m				
		Inlet	Outlet	Top	Bottom	Sides
ITTC 2011 [24]	Cargo ship	L_{OA}	$5L_{OA}$	$0.5L_{OA}$	$2L_{OA}$	$2L_{OA}$
Tran Gia Thai et al [28]	Wooden Fishing vessel	$2L_{pp}$	$4L_{pp}$	L_{pp}	L_{pp}	$2L_{pp}$
Yigit Kemal Demiret [22]	All type of ship	$1.5L_{pp}$	$2.5L_{pp}$	$1.5L_{pp}$	$2.5L_{pp}$	$2.5L_{pp}$

In the case study, the initial size variant of the computational domain of the FAO 75 model is variant 1 in Table 3. The distance between the inlet boundary and ship model will be changed first from $2L_{PP}$ value to $1.5L_{PP}$ value while the positions of the remaining boundaries are kept unchanged corresponding to variant 2 in Table 3. The CFD-based resistance value under variant 2 is significantly increased compared to the resistance value of the initial variable shown that the position of Inlet boundary, in this case, is located too close to the ship model which increases the resistance due to the appearance of the reverse wave system by the boundary wall effect. The CFD-based resistance result is unchanged in variant 3, which corresponds with increasing the initial distance of the inlet boundary to $2.5L_{PP}$ value, shown that $2L_{PP}$ is the appropriate distance of the inlet boundary in this case. The appropriate distances for the remaining boundaries have been obtained by performing the same calculations. Variant 5 and variant 7 in Table 3 are corresponding to the appropriate distances of outlet and side boundaries. To reduce the calculation variants, the Top and Bottom boundaries in all variants of the computational domain are unchanged because they are usually quite identical in most of the recommendations and haven't much affected the result of resistance.

TABLE III
SIZE VARIANTS OF COMPUTATION DOMAIN AND CORRESPONDING RESISTANCE VALUES

Variant	Size and boundary positions of computational domain					Resistance values
	Inlet	Outlet	Sides	Top	Bottom	
1	$2L_{pp}$	$5L_{pp}$	$2.5L_{pp}$	L_{pp}	L_{pp}	6382.02
2	$1.5L_{pp}$	$5L_{pp}$	$2.5L_{pp}$	L_{pp}	L_{pp}	6421.38
3	$2.5L_{pp}$	$5L_{pp}$	$2.5L_{pp}$	L_{pp}	L_{pp}	6382.03
4	$2L_{pp}$	$4L_{pp}$	$2.5L_{p}$	L_{pp}	L_{pp}	6382.03
5	$2L_{pp}$	$3L_{pp}$	$2.5L_{pp}$	L_{pp}	L_{pp}	6382.04
6	$2L_{pp}$	$2.5L_{pp}$	$2.5L_{pp}$	L_{pp}	L_{pp}	6276.32
7	$2L_{pp}$	$3L_{pp}$	$2L_{pp}$	L_{pp}	L_{pp}	6382.24
8	$2L_{pp}$	$3L_{pp}$	$1.5L_{pp}$	L_{pp}	L_{pp}	6261.36

As the calculation results in Table 3, it can be obtained an appropriate size of computation domain for the given model is the variant with a distance of 2LPP in front of the model, a distance of 3LPP behind the model, and a same distance of LPP for the top, bottom and two sides of the model as shown in the Figure 4.

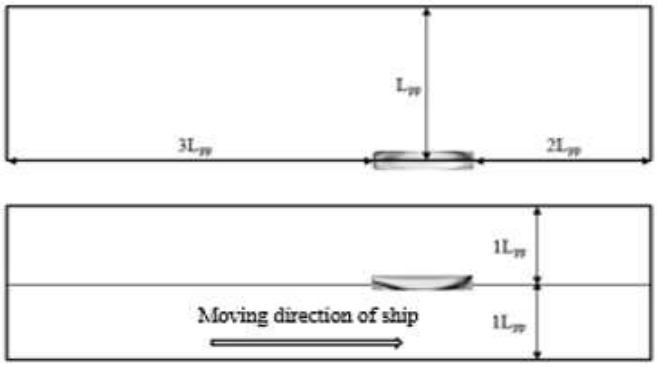

Fig. 4 Size of computation domain under the given ship model

B. Determining the Appropriate Turbulent Model

As above presented, the known turbulent model SST k-ω has been usually used to predict ship resistance. The theatrical approach of determining these parameters by the characteristics of the given hull form is presented based on flowing the empirical equations [18]:

$$k = \frac{3}{2}(IU_F)^2 \quad (1)$$

$$\varepsilon = \frac{\sqrt{k}}{L_{PP}} \quad (2)$$

$$\omega = \frac{\varepsilon}{k} \quad (3)$$

where I is turbulent intensity that is determined according to the empirical values: I is less than 1.00 for slow speed ships, I is from 0.01 to 0.10 for medium speed ships, and I is more significant than 1.00 for high-speed ships; U_F is the speed of flow determined equal to speed of ship, m/s; L_{PP} is the length between perpendiculars, m; k is the turbulent kinetic energy; ω is the specific rate of dissipation; ε is the rate of dissipation of turbulent kinetic energy.

Based on above empirical equations, it is put forward a practical approach to determine the appropriate values of the parameters of turbulence kinetic energy k and turbulence energy ω of turbulent model SST k-ω for the specific ship type as following: Preliminary estimating some initial values of turbulent intensity I within its range following the speed of the given hull to calculate the corresponding values of k and ω parameters based on the above empirical equations.

Computing the resistance of the given ship model for all parameter variant of turbulent model (I, k, ω) using CFD and comparing with the corresponding model test results to find the appropriate parameter variant of turbulent model based on ensuring the deviation between the resistance values obtained from CFD and model test are minimum and in the given limit. It is usually less than 3%.

In case of study, FAO 75 vessel is designed at the medium speed U_F = 15 knots = 7.713 m/s and the length between perpendiculars L_{PP} = 44.2 m so it can be set up the initial variant of the turbulent model with the value of turbulent intensity I equal to 0.010 and calculated values of k and ω equal to 0.009 and 0.240 respectively. The computational results and comparison of resistance values under all parameter variants of the turbulent model of FAO 75 model obtained from OpenFOAM and from the model test are presented in Table 4.

TABLE IV
THE COMPUTATIONAL RESULTS AND COMPARISON OF RESISTANCE VALUES UNDER ALL PARAMETER VARIANTS OF THE TURBULENT MODEL OF FAO 75 MODEL OBTAINED FROM OPENFOAM AND FROM MODEL TEST

FAO 75: L_{pp} = 44.2 m ; U = 15 hl/h = 7.71 m/s ; R_{tn} = 15743.9 KG											
I	0.01	0.03	0.05	0.052	0.054	0.056	0.058	0.06	0.07	0.08	0.10
k	0.009	0.080	0.223	0.241	0.260	0.280	0.300	0.321	0.437	0.571	0.892
ε	0.002	0.006	0.011	0.011	0.012	0.012	0.012	0.013	0.015	0.017	0.021
ω	0.240	0.080	0.048	0.046	0.044	0.043	0.041	0.040	0.034	0.030	0.024
R_{XF} (KG)	13016.2	14061.2	14523.3	15543.5	16241.5	16674.7	16832.4	17854.3	17976.4	16816.8	18244.2
ΔR (%)	-17.33	-10.69	-7.75	-1.27	3.16	5.91	6.91	13.40	14.18	6.81	15.88

Figure 5 shows the graphics of the flow field around FAO 75 hull in the initial variant and the chosen variant. It is easy to find that the flow field around in the initial variant (figure 5a) is quite unstable and tangled firmly together with its wave system is broken even it is far from a ship model when compared to the flow field around in the chosen variant (Figure 5b).

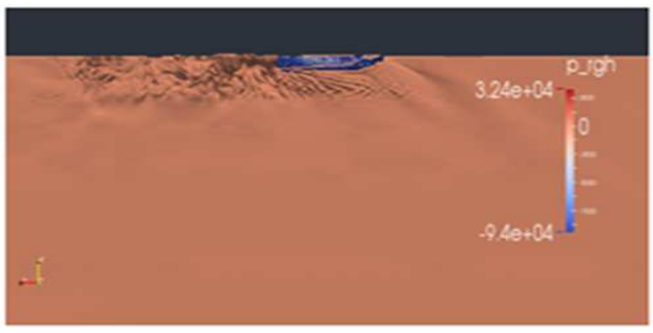

(a) I = 0.010, k = 0.009, ω = 0.240

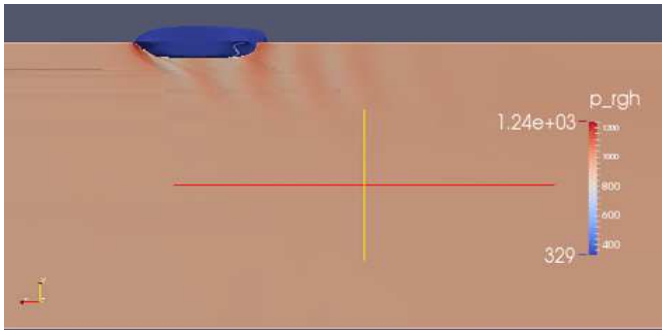

(b) I = 0.052, k = 0.241, ω = 0.046

Fig. 5 Flow field around the computation model is in two study cases

Figure 6 presents the convergent rate of the CFD solution for resistance prediction of the FAO 75 model in two above variants. In the initial variant, the convergent rate of CFD solution is quite slow as shown in figure 4a and the CFD-based resistance value is quite different from the model test. All these results are explained by the mismatch of the turbulent model parameters with the hull geometry. In the chosen variant, the convergent rate of CFD solution for resistance prediction is quite fast corresponding to the number of iterations about 4000 steps, as shown in figure 6b. This allows us to conclude that the chosen parameters of the turbulent model are to suit the geometry of the computational hull.

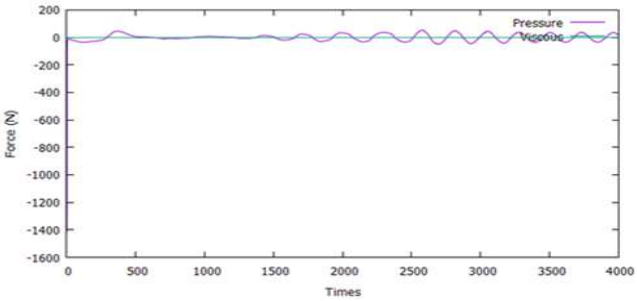

(a) I = 0.010, k = 0.009, ω = 0.240

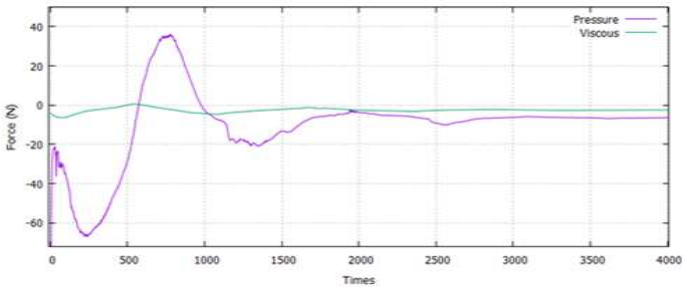

(b) I = 0.052, k = 0.241, ω = 0.046

Fig. 6 The convergent rate of the CFD solution for the resistance prediction of FAO 75 model in two study cases

C. The Accuracy and Reliability of the Proposed Approach

The resistance prediction of FAO 75 fishing vessels under the different Froude numbers was performed with the chosen value of the input parameters to evaluate the accuracy and reliability of the proposed approach. The same computational procedure of resistance prediction was performed for the fishing vessel named FAO 72 that has similar geometric characteristics to FAO 75 fishing vessels and tested in the towing tank by FAO. The CFD-based resistance results of FAO 72 and FAO 75 vessel under the above-chosen input parameters can be found in [1] in which their resistance values and curves are described in Table 5 and Figure 7 respectively. These computational results are a reliable evidenced for the accuracy and reliability of the proposed approach, in which all deviation between the CFD-based (R_{CFD}) and model tests (R_{tn}) resistance values are less than 5%.

TABLE V

THE COMPUTATION RESULTS AND DEVIATIONS BETWEEN CFD-BASED AND MODEL TEST VALUES OF RESISTANCE OF FAO 72 AND FAO 75 HULLS

Fn	U (m/s)	I	k	ω	FAO 72			FAO 75		
					R_X (KG)	R_{tn} (KG)	ΔR_{72} (%)	R_X (KG)	R_{tn} (KG)	ΔR_{75} (%)
0.150	3.123	0.052	0.044	0.707	1439.07	1497.30	-4.05	1501.31	1501.50	-0.01
0.175	3.644	0.052	0.060	0.824	1711.07	1765.90	-3.20	1640.49	1606.18	2.09
0.200	4.165	0.052	0.079	0.942	2360.17	2386.10	-1.10	2294.45	2252.25	1.84
0.225	4.685	0.053	0.100	1.060	3129.52	3242.10	-3.60	3106.69	3003.00	3.34
0.250	5.206	0.053	0.123	1.178	4519.34	4639.90	-2.67	4619.56	4504.51	2.49
0.275	5.726	0.053	0.149	1.296	5291.31	5513.00	-4.19	5806.90	5733.01	1.27
0.300	6.247	0.053	0.002	1.413	6437.01	6550.90	-1.77	6367.15	6381.38	-0.22
0.325	6.768	0.054	0.002	1.531	7596.12	7774.60	-2.35	7568.37	7623.01	-0.72
0.350	7.288	0.054	0.003	1.649	10250.87	10587.90	-3.29	10321.11	10617.76	-2.87
0.375	7.809	0.054	0.003	1.767	15131.38	15571.60	-2.91	17287.12	16816.82	2.72
0.400	8.329	0.052	0.004	1.837	24176.59	23322.90	3.53	22946.64	23244.17	-1.30

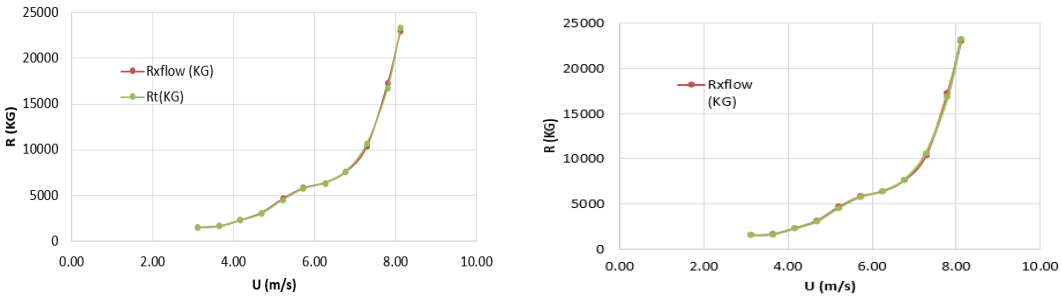

FAO 72 FAO 75

Fig. 7 A comparative on resistance curves that are determined on CFD-based and model test of FAO 72 and FAO 75 hulls

IV. CONCLUSION

The objective of the approach is to improve the accuracy of CFD-based resistance values of a specific ship based on adjusting the input parameters of the CFD solution for resistance prediction according to the geometric characteristics of the given hull. The following conclusions are drawn from these research results:

The accuracy of three dimensions (3D) model of computational ship: The accuracy of the 3D model is one of the important input factors to improve the accuracy of resistance values. The solution of using the ship design software as Autoship software to create and adjust based on comparing the geometric parameters of the 3D model with the corresponding real ship are appropriate to ensure the required accuracy of the CFD solution for resistance prediction on the given hulls.

The appropriate input parameters of CFD solution for the resistance prediction of fishing vessels: The appropriate values of the input parameters, including computational domain size and turbulent model parameters for resistance prediction using CFD of FAO 75 vessel shown in Figure 3 and Table 3 respectively. These figures will provide a valuable reference relating to determining the value of the input parameters for CFD-based resistance prediction of fishing vessels with the same geometric characteristics as FAO 75 vessel.

Also from the calculation results in Table 3, it can be chosen the values of turbulent intensity (I) depending on speed and geometric characteristics of the given hull type of fishing vessels as following: I= 0.052 when Fn $\leq$ 0.20; I = 0.053 when 0.20 < Fn < 0.30; I= 0.054 when Fn $\geq$ 0.30. In our reviewing and evaluating, the supposed value of turbulent intensity (I) is slightly higher than usual. This leads the value of the parameter (k) is higher and the value of the parameter (ω) is smaller than the current cargo ship. For example, the calculation value of parameters (k) and (ω) for the Kriso Container Ship (KCS), which is often used as the computational ship for the numerical simulation researches equal to 0.00015 and 2.00 respectively. This can be explained by the geometric characteristics of the hull type of fishing vessels in this research. They have not a good hydrodynamic form with a sort cylindrical part and usually operate in working regimes with relatively large Froude numbers Fn = (0.35 - 0.40) when comparing with the conventional cargo ships. So, most fishing vessels usually operate in the mode of generating high wave energy that leads to the values of the turbulent intensity (I) and turbulence kinetic energy (k) is higher than the others.

REFERENCES

[1] Y. Chi and F. Huang, "An overview of the simulation-based hydrodynamic design of ship hull forms," *J. Hydrodyn. Ser. B*, vol. 28, no. 6, pp. 947–960, 2016.

[2] A. Lungu, "Trial computations of the free-surface flow around a bulk carrier ship model," *Ann. of" Dunarea Jos" Univ. Galati. Fascicle XI Shipbuilding.*, vol. 39, pp. 73–80, 2016.

[3] A. T. Hoang and V. V. Pham, "Impact of jatropha oil on engine performance, emission characteristics, deposit formation, and lubricating oil degradation," *Combust. Sci. Technol.*, vol. 191, no. 03, pp. 504–519, 2019.

[4] J. Wang, L. Zou, and D. Wan, "Numerical simulations of zigzag maneuver of the free-running ship in waves by RANS-Overset grid method," *Ocean Eng.*, vol. 162, pp. 55–79, 2018.

[5] C. H. Son, "CFD Investigation of Resistance of High-Speed Trimaran Hull Forms." 2015.

[6] A. T. Hoang and V. V. Pham, "A study of emission characteristics, deposits, and lubrication oil degradation of a diesel engine running on preheated vegetable oil and diesel oil," *Energy Sources, Part A Recover. Util. Environ. Eff.*, vol. 41, no. 5, pp. 611–625, 2019.

[7] S. Lee and C. Hong, "Study on the course stability of very large vessels in shallow water using CFD," *Ocean Eng.*, vol. 145, pp. 395–405, 2017.

[8] M. Diez, R. Broglia, D. Durante, A. Olivieri, E. Campana, and F. Stern, "Validation of uncertainty quantification methods for high-fidelity CFD of ship response in irregular waves," in *55th AIAA Aerospace Sciences Meeting*, 2017, p. 1655.

[9] L. Du, H. Hefazi, and P. Sahoo, "Rapid resistance estimation method of non-Wigley trimarans," *Ships Offshore Struct.*, pp. 1–11, 2019.

[10] H. Chang, X. Cheng, Z. Liu, B. Feng, and C. Zhan, "Sample selection method for ship resistance performance optimization based on the approximated model," *J. Sh. Res.*, vol. 60, no. 1, pp. 1–13, 2016.

[11] S. Zhang, B. Zhang, T. Tezdogan, L. Xu, and Y. Lai, "Computational fluid dynamics-based hull form optimization using approximation method," *Eng. Appl. Comput. Fluid Mech.*, vol. 12, no. 1, pp. 74–88, 2018.

[12] W. Luo and L. Lan, "Design Optimization of the Lines of the Bulbous Bow of a Hull Based on Parametric Modeling and Computational Fluid Dynamics Calculation," *Math. Comput. Appl.*, vol. 22, no. 1, p. 4, 2017.

[13] J. Yao, W. Jin, and Y. Song, "RANS simulation of the flow around a tanker in forced motion," *Ocean Eng.*, vol. 127, pp. 236–245, 2016.

[14] P. Akbarzadeh, P. Molana, and M. A. Badri, "Determining resistance coefficient for series 60 vessels using numerical and experimental modeling," *Ships Offshore Struct.*, vol. 11, no. 8, pp. 874–879, 2016.

[15] L. Leal, E. Flores, D. Fuentes, and B. Verma, "Hydrodynamic study of the influence of bulbous bow design for an Offshore Patrol Vessel using Computational Fluid Dynamics," *Sh. Sci. Technol.*, vol. 11, no. 22, pp. 29–39, 2018.

[16] T. Tezdogan, Y. K. Demirel, P. Kellett, M. Khorasanchi, A. Incecik, and O. Turan, "Full-scale unsteady RANS CFD simulations of ship behavior and performance in head seas due to slow steaming," *Ocean Eng.*, 2015.

[17] S.-E. Kim *et al.*, "A Scalable and Extensible Computational Fluid Dynamics Software Framework for Ship Hydrodynamics Applications: NavyFOAM," *Comput. Sci. Eng.*, vol. 19, no. 6, pp. 33–39, 2017.

[18] Y. Liu, L. Zou, and Z.-J. Zou, "Computational fluid dynamics prediction of hydrodynamic forces on a maneuvering ship including effects of dynamic sinkage and trim," *Proc. Inst. Mech. Eng. part M J. Eng. Marit. Environ.*, vol. 233, no. 1, pp. 251–266, 2019.